https://doi.org/10.5194/egusphere-2026-2501
Preprint. Discussion started: 22 May 2026

Multi-Data Source Based Quantifying Urban Flood Severity in Major Chinese Cities (2000 – 2024) Using a Hybrid Machine-Learning Weighting Framework

Guoqiang Peng[1], Yujing Sun[1], Mao Wang[1], Min Chen[2], Fengyuan Zhang[2]

[1]School of Geography and Tourism, Shaanxi Normal University, Xi'an, China, 710119
[2]School of Geography, Nanjing Normal University, Nanjing, China, 210023

Correspondence to: Yujing Sun (syj1011@snnu.edu.cn)

Abstract. Urban flooding poses a major challenge to sustainable urban development, yet most existing assessments focus on single cities or river basins and rely on limited historical records. This study integrates multi-source data from 20 Chinese cities over 2000–2024 to develop a comparable long-term assessment of urban flood severity. To address the fragmentation and inconsistency of flood evidence across official records, news reports, and social media, we construct an event-level database and derive a Flood Severity Index (FSI) using an interpretable data-driven weighting and ensemble framework. Robustness is evaluated through repeated resampling and consistency checks across cities and years. The results show that southern cities experience more frequent and severe flooding, whereas northern cities are generally less affected but more vulnerable to abrupt extremes. These findings suggest distinct governance priorities: reducing chronic exposure in southern cities and strengthening preparedness for high-impact shocks in northern cities. The proposed framework is transferable to other regions and provides a basis for future cross-regional flood risk comparison and adaptive urban risk governance.

1 Introduction

Global climate change and rapid urbanization have led to a significant increase in the frequency and intensity of urban flood events (Rentschler et al., 2023). As one of the most destructive natural hazards in urban areas (Bagheri et al., 2025), urban flooding has become a major barrier to achieving global sustainable development goals (Xu et al., 2023). Urban flood impacts are jointly driven by hydroclimatic extremes and urban development processes, producing substantial spatial heterogeneity and temporal variability (Yin et al., 2016; Wu et al., 2020; Qi et al., 2024). A comprehensive understanding of the spatial and temporal evolution of flood severity, together with a critical review of existing research, is therefore essential for informing future planning, enhancing disaster prevention and mitigation capacity, and improving urban resilience (Sanders et al., 2023).

In urban flood research, assessment has increasingly adopted a multi-scale framework spanning micro-scale process simulation, macro-scale risk characterization, and near-real-time decision support. At the micro scale, physically based hydrodynamic models (e.g., SWMM and MIKE21) are widely used to reproduce urban inundation dynamics at high

https://doi.org/10.5194/egusphere-2026-2501
Preprint. Discussion started: 22 May 2026

spatiotemporal resolution (Bhusal et al., 2024; Yang et al., 2020). Recent work further improves surface routing and backflow representation through coupled frameworks, enhancing simulations of inundation extent, depth, and duration (Yang et al., 2023). At broader spatial scales, from cities to regions, research has expanded from hazard mapping to integrated assessments that jointly consider hazard, exposure, and vulnerability (Wing et al., 2020), often implemented through multi-indicator frameworks combined with GIS and MCDA (Chen et al., 2024). For example, spatiotemporal flood risk in Zhengzhou (2005–2020) has been examined by integrating Random Forest with MCDA (Li et al., 2023), whereas flood resilience has been evaluated by combining Random Forest and Support Vector Machine models with the Analytic Hierarchy Process (Hussain et al., 2023). Regional frameworks have also applied hybrid weighting methods to synthesize hazard severity, environmental exposure, and socio-economic vulnerability (Peng et al., 2022), and GIS–MCDA has been used to assess flood susceptibility in data-scarce regions (Ahmad et al., 2025; Xu et al., 2024). Meanwhile, data-driven approaches for flood monitoring, early warning, and emergency response have become major research hotspots. With advances in remote sensing, social media analytics, and artificial intelligence (Dai et al., 2024; Tellman et al., 2021), near-real-time flood monitoring and decision support for emergency management are increasingly feasible (Zhang et al., 2023; Misra et al., 2025). Social media data enable rapid flood classification and post-disaster monitoring (Tan et al., 2021). Moreover, multimodal frameworks fusing remote-sensing imagery with textual data provide more intuitive and quantitative grounded representations of urban flood vulnerability (Duan et al., 2024).

Although large-scale studies have examined flood vulnerability and human–environment interactions (Ban et al., 2023; Rogers et al., 2025), research that uses flood events to reveal inter-city differences in flood responses and their links to divergent urban development patterns remains limited. This gap is underscored by recent catastrophic urban flood events—such as the 2021 Zhengzhou rainstorm–flood and major flood events in Beijing—in which severe inundation contributed to substantial casualties, highlighting the urgency of systematically comparing how different cities experience, absorb, and recover from flood disasters. This gap can be attributed to three main limitations. First, most studies focus on individual river basins (e.g., the Yangtze River, the Pearl River) or megacities (e.g., Beijing, Shanghai), and systematic cross-regional comparisons among cities of different sizes and geographic characteristics are largely lacking. This limitation constrains the identification of universal patterns and regional disparities in urban flood risk (Guo et al., 2021; Jiang et al., 2018; Li et al., 2023). Second, existing evaluation frameworks for flood severity remain incomplete. Many frameworks primarily emphasize hazard-inducing factors (e.g., extreme rainfall), whereas quantitative analyses of vulnerability—particularly economic losses, affected area, and social impacts—are still insufficient (Li et al., 2025). As a result, the integrated severity of urban flood disasters is not fully captured. Third, long-term disaster datasets remain scarce. Many studies rely on short, fragmented records or simulated events (Zhang et al., 2025), while multi-decadal, event-based urban flood databases that combine official statistics, documentary records, and social media information are still rare (Cao et al., 2022; Romali et al., 2025).

To address these gaps, this study develops a unified framework to evaluate and compare urban flood disaster severity across 20 representative cities in northern and southern China from 2000 to 2024. This effort is motivated by the need for (1) consistent, long-term and comparable evidence across cities assembled from fragmented records, (2) a more robust and

https://doi.org/10.5194/egusphere-2026-2501
Preprint. Discussion started: 22 May 2026

interpretable severity assessment that can account for nonlinear indicator–impact relationships beyond conventional linear weighting schemes, and (3) a systematic understanding of how flood severity has evolved and diverged between northern and southern China to support differentiated mitigation and resilience planning. The study focuses on severity evaluation and spatiotemporal pattern identification; the explicit quantification of long-term effects of urban water-body evolution on flood severity is reserved for future research building on the framework established here.

2 Materials

2.1 Study area

To support a north–south comparison of urban flood severity, this study delineates a Northern Urban Region (NUR) (34° N–41° N, 112° E–122° E; mainly north of the Qinling–Huaihe Line) and a Southern Urban Region (SUR) (28° N–32° N, 110° E–122° E; Yangtze River Delta and surrounding cores). Because total GDP is strongly correlated with population size and urban extent and thus reflects development intensity, the top ten cities by GDP were selected in each region (Hu et al., 2024; Fang et al., 2026). The NUR features a temperate monsoon climate with dry winters and concentrated summer rainfall. Water resources are uneven and generally scarce, placing cities under combined pressures of water scarcity and flood risk (Luo et al., 2023). The northern cities are Beijing, Tianjin, Qingdao, Zhengzhou, Jinan, Xi'an, Yantai, Tangshan, Shenyang, and Dalian. Sponge-city initiatives and drainage upgrades have been promoted, yet coping with climate change–driven extremes remains challenging under rapid urbanization and rigid water constraints (Yin et al., 2021; Liu et al., 2022). The SUR has a subtropical monsoon climate, abundant precipitation, and dense river networks, and is highly exposed to typhoons, torrential rainfall, and basin-scale floods (Wang, P. et al., 2022), as illustrated by the 2020 Yangtze flooding impacts in Wuhan (Ge et al., 2023). The southern cities are Shanghai, Shenzhen, Guangzhou, Wuxi, Chengdu, Suzhou, Hangzhou, Wuhan, Nanjing, and Ningbo. Despite relatively strong flood-control capacity, long-term pressures persist due to sea-level rise, intensified extremes, surface hardening, and the "rain island effect" (Liang et al., 2016). Chongqing (GDP rank 9) was excluded because persistent fog degrades remote-sensing imagery; Wuxi (rank 11) was substituted (Fig. 1).

https://doi.org/10.5194/egusphere-2026-2501
Preprint. Discussion started: 22 May 2026

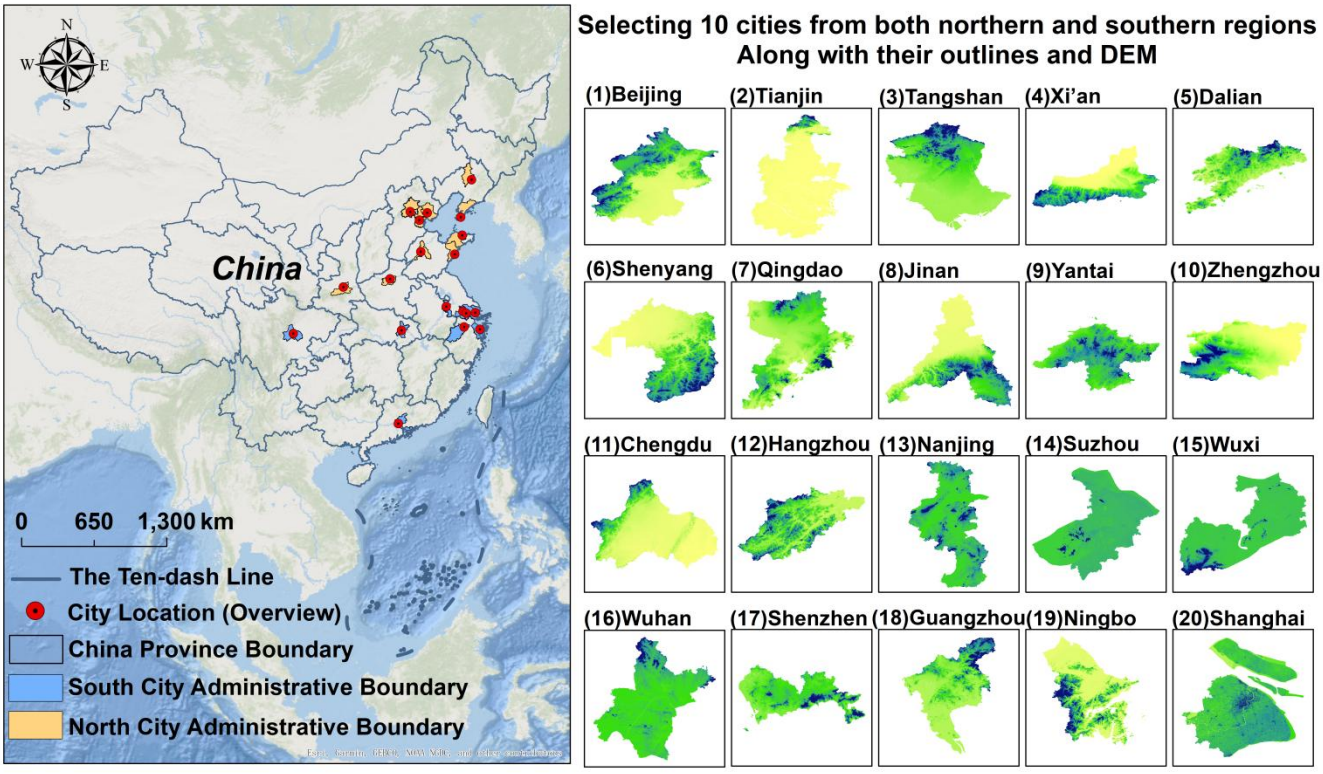

Figure 1: Study area and geographical distribution of the 20 sample cities.

2.2 Data Sources and Processing

2.2.1 Data sources

The flood disaster data used in this study were primarily obtained from two sources: social media text data and authoritative news reports.

A Python-based web crawler was employed to systematically collect flood-related public posts from the Sina Weibo platform, using keywords such as "urban waterlogging," "rainstorm flooding," "road inundation," and "drainage congestion." The collected dataset covered 2010–2024 and included text content, posting time, geographic location, and user attributes. Natural language processing (NLP) techniques were applied for semantic filtering and noise reduction, thereby removing advertisements, duplicate records, and irrelevant content, while retaining valid flood event records (Fu et al., 2025). In addition, data from authoritative news media and official government websites—including Statistical Yearbooks, Xinhua News Agency, China Weather Network, People's Daily, and announcements from local flood control and emergency management departments—were used to verify the authenticity and spatiotemporal consistency of flood events reported on social media (Fu et al., 2025). These data served as reliable references for corroborating social media information (2010–

https://doi.org/10.5194/egusphere-2026-2501
Preprint. Discussion started: 22 May 2026

2024). For the period prior to social media coverage (2000 – 2009), the database relied primarily on authoritative documentary sources and official records.

To reflect public attention and information dissemination trends regarding flood events, Baidu Index and Google Trends were used to quantify online public interest. The spatial and temporal variations in public concern were measured by analyzing the search popularity of related keywords (e.g., “urban waterlogging” and “rainstorm disasters”) over specific time periods.

2.2.2 Dataset construction and interpolation

Based on the above data sources, a comprehensive urban flood disaster database was developed to cover the sample cities. The database includes key attributes such as event occurrence time, location (latitude and longitude), fatalities, affected area, affected population, economic losses, and online attention indices. To ensure data completeness, missing attribute values (e.g., economic losses or affected population) for confirmed flood events were imputed using statistical methods. This procedure was used only to fill missing values in existing event records; no artificial flood events were generated for periods with no documented disasters. Due to limitations in data collection, some years in certain cities had no available records.

The final flood disaster database integrates multi-source spatiotemporal information, social sentiment data, and disaster intensity indicators, thereby providing a robust data foundation for subsequent flood severity assessment, spatial modeling, and comprehensive evaluation.

3 Methods

3.1 Research framework

As illustrated in Fig. 2, the overall research framework consists of four sequential stages:

(1) Data preparation and indicator construction: The raw data were cleaned and standardized, and a Flood Severity Index (FSI) was constructed for model training.

(2) Model evaluation: Multiple machine learning algorithms were trained to perform regression and classification tasks, and model robustness was evaluated through cross-validation and consistency testing (Wang et al., 2024).

(3) Hybrid weighting and interpretability analysis: Expert knowledge was integrated with machine learning optimization, and the SHAP method was used to interpret model behavior (Zhao et al., 2024).

(4) Spatiotemporal analysis: The final model results were utilized to evaluate flood severity across cities and years, thereby revealing the spatiotemporal variation in flood severity.

This design mitigates limitations of both traditional MCDA and purely data-driven approaches. AHP/EWM frameworks rely on fixed linear weights and may fail to capture nonlinear relationships and cross-indicator interactions, whereas black-box ML models may not adequately incorporate expert knowledge and lacks transparent attribution. Here, ML serves as a

https://doi.org/10.5194/egusphere-2026-2501
Preprint. Discussion started: 22 May 2026

nonlinear mapping module to capture complex relationships, with AHP/EWM retained as interpretable baselines for comparison and plausibility checks.

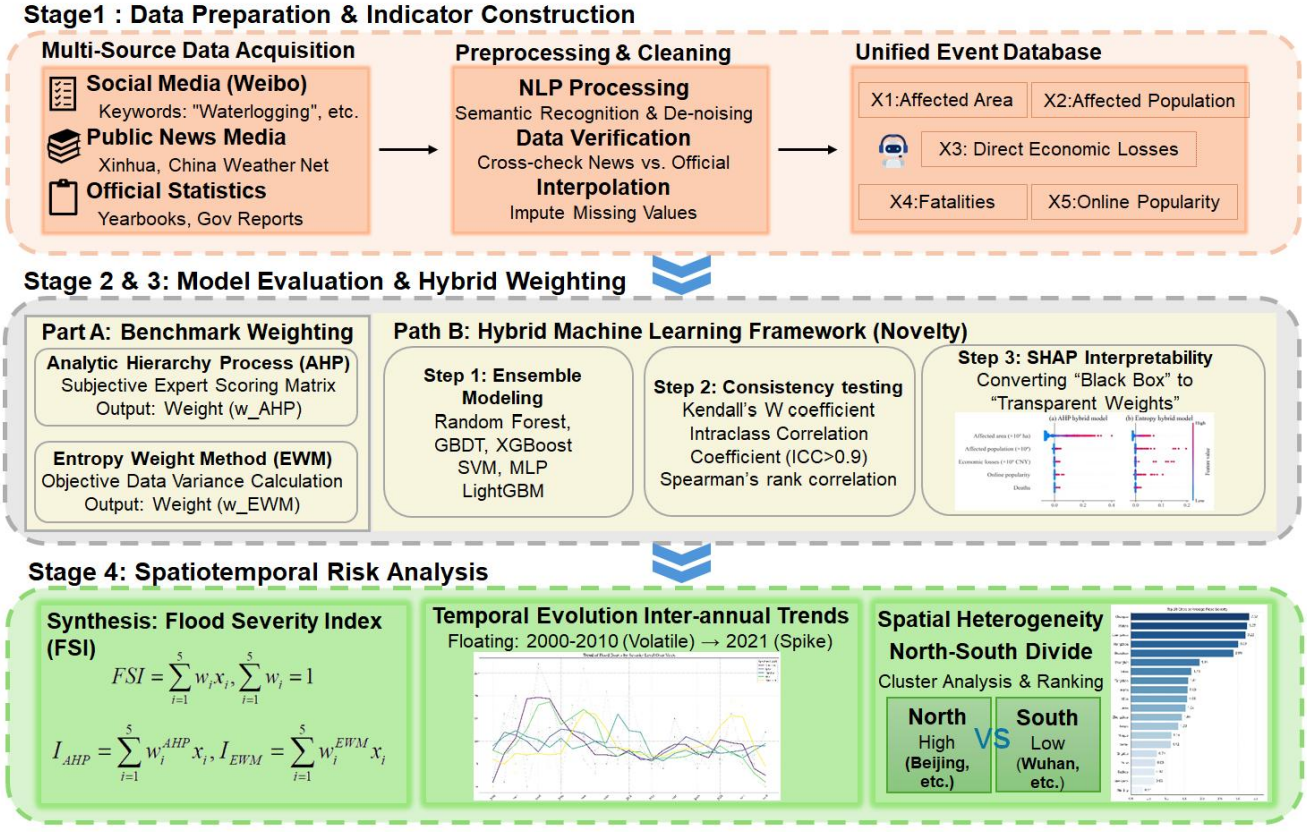

Figure 2: Flowchart of the hybrid machine learning-based weighting framework.

3.2 Data preprocessing

The raw dataset was cleaned to address missing values, standardize column names, and harmonize city identifiers. To eliminate differences in sacle and magnitude among variables, two scaling methods were applied:

(1) MinMaxScaler: Data were scaled to the range [0, 1], primarily for constructing the Flood Severity Index (FSI).

(2) StandardScaler: Variables were standardized to have a mean of 0 and a standard deviation of 1, thereby enhancing model convergence and stability.

3.3 Construction and classification of the Flood Severity Index (FSI)

To support both severity evaluation and supervised learning, two types of target variables were generated.

(1) In this study, a continuous Flood Severity Index (FSI) was developed to quantify the overall impact of each flood event. The FSI was defined as a weighted linear combination of five core indicators that represent physical, socio-economic and

https://doi.org/10.5194/egusphere-2026-2501
Preprint. Discussion started: 22 May 2026

perceptual dimensions of flood impacts. These indicators include affected area (x_1), affected population (x_2), direct economic losses (x_3), fatalities (x_4) and online popularity (x_5). All variables were normalized to the range [0,1]. The flood severity index (FSI) was defined according to Eq. (1).

$$FSI = \sum_{i=1}^{5} w_i x_i, \sum_{i=1}^{5} w_i = 1 \quad (1)$$

where w_i denotes the weight of each indicator.

Two sets of weights were derived using the expert-based Analytic Hierarchy Process (AHP) and the objective Entropy Weight Method (EWM), respectively. Accordingly, two composite indices were calculated for each flood event as expressed in Eq. (2).

$$I_{AHP} = \sum_{i=1}^{5} w_i^{AHP} x_i, I_{EWM} = \sum_{i=1}^{5} w_i^{EWM} x_i \quad (2)$$

These two indices serve as benchmarks for comparative analysis with the ML-derived index. Instead of directly fixing the indicator weights based on AHP or EWM, this design allows the models to flexibly recalibrate the relative contributions of exposure, losses, fatalities, and online attention, thereby reducing the risk of bias introduced by subjective judgment or limited sample variance.

(2) A discrete flood severity level was derived using a quantile-based discretization approach, which divided the continuous FSI into five categories—very low, low, medium, high, and very high—serving as the dependent variable for classification models.

3.4 Machine learning model evaluation

Six representative machine learning algorithms were selected for comparative evaluation, including Random Forest (RF), Gradient Boosting Decision Tree (GBDT), XGBoost, LightGBM, Support Vector Machine (SVM), and Multi-Layer Perceptron (MLP) (Wu et al., 2020). Model performance was comprehensively evaluated from three complementary perspectives:

(1) Predictive performance: assessed using 10-fold cross-validation, with R^2 for regression tasks and Accuracy/F1-score for classification tasks.

(2) Training behavior: analyzed through learning curves to detect overfitting and evaluate model stability.

https://doi.org/10.5194/egusphere-2026-2501
Preprint. Discussion started: 22 May 2026

(3) Consistency testing: performed using Kendall's W coefficient, the intraclass correlation coefficient (ICC), and Spearman's rank correlation to verify the consistency of model results and feature importance rankings across algorithms.

3.5 Hybrid weighting determination and model interpretability

To integrate expert knowledge and data-driven learning, this study adopted a hybrid weighting strategy. However, unlike traditional supervised learning where models predict a pre-defined label, here machine learning is utilized as a nonlinear weighting mechanism.

Instead of using the AHP- or EWM-derived FSI as a target variable for prediction—which would imply circular reasoning—we employ tree-based ensemble algorithms (Random Forest, GBDT, XGBoost, and LightGBM) to capture the intrinsic data structure and the nonlinear interactions among the five core indicators (x_1-x_5). For each model, the training process is leveraged to derive indicator contribution scores using SHapley Additive exPlanations (SHAP). These global importance scores are then normalized to generate a set of non-negative, data-driven weights (w_i^{ML}) such that $\sum w_i^{ML} = 1$. Consequently, the Machine-Learning-based Flood Severity Index (FSI_{ML}) is calculated as a weighted linear combination of the selected indicators, as expressed in Eq. (3).

$$FSI_{ML} = \sum_{i=1}^{5} w_i^{ML} x_i \tag{3}$$

This design transforms the "black box" models into transparent weighting generators. It allows for a consistent comparison between the subjective AHP-derived patterns (FSI_{AHP}), the objective EWM-derived patterns (FSI_{EWM}), and the nonlinear ML-derived patterns (FSI_{ML}), providing a robust and interpretable assessment of flood severity without relying on potentially biased ground-truth labels.

3.6 Spatiotemporal analysis and risk attribution

Based on the ML-derived flood severity index (FSI_{ML}), the spatiotemporal pattern of flood severity was analyzed.

At the urban level, the mean severity level and the proportion of high-risk events were calculated to construct a ranking for 20 cities. At the temporal level, the interannual frequency and temporal trends of different severity categories were examined. To explore spatial heterogeneity, the cities were grouped into northern and southern clusters, and the two groups were compared in terms of severity evolution and resilience.

https://doi.org/10.5194/egusphere-2026-2501
Preprint. Discussion started: 22 May 2026

4 Results

4.1 Model performance

To ensure that the subsequent spatial–temporal analyses are credible, this section first evaluates the plausibility of the weight distribution, internal consistency, and interpretability of the proposed hybrid weighting–machine-learning framework.

4.1.1 Distribution of data-driven weights

The feature importance scores derived from six machine learning algorithms (RF, GBDT, XGBoost, LightGBM, SVM, and MLP) were normalized to obtain the data-driven weights (w^{ML}). Unlike methods such as AHP, which rely on subjective expert hierarchy, or the Entropy Weight Method (EWM), driven solely by statistical variance, the w^{ML} weights capture the nonlinear contribution of each indicator to the intrinsic structure of flood severity. In contrast to the EWM, which tends to over-emphasize indicators with high volatility (such as economic losses), and the AHP method, which seeks a more balanced allocation of weights, the machine learning-derived weights consistently highlight "Affected Area" (x_1) and "Affected Population" (x_2) as the most critical drivers. This suggests that, within the underlying data structure, spatial scale and demographic impact are the most robust indicators for distinguishing severity levels. These findings not only align with physical intuition but are also supported by data-driven learning.

4.1.2 Cross-model consistency

To assess robustness, three complementary consistency diagnostics were applied to the six hybrid models.

First, Kendall's W was used to evaluate the concordance of feature-importance rankings across the models. Significant agreement was observed for both weighting schemes (AHP: $W \approx 0.7181$, entropy weighting: $W \approx 0.7204$, both $p < 0.001$), indicating that, despite differences in algorithmic structure, the models converge in identifying the variables that most strongly influence flood severity.

Second, pairwise Spearman rank correlations of the predicted severity rankings revealed uniformly high and statistically significant correlations among the six models, demonstrating that the models produce highly consistent severity rankings across the event set, as shown in Fig. 3.

Third, the intraclass correlation coefficient (ICC) was calculated by treating the six models as a fixed set of raters. The average-measure coefficient reached an excellent level (ICC(3,k) = 0.920, 95% CI [0.91, 0.93], $p < 0.001$), providing quantitative evidence that the hybrid models yield highly reliable and reproducible estimates of flood severity.

Taken together, these results show that the hybrid framework is not only robust but also internally consistent across algorithms.

https://doi.org/10.5194/egusphere-2026-2501
Preprint. Discussion started: 22 May 2026

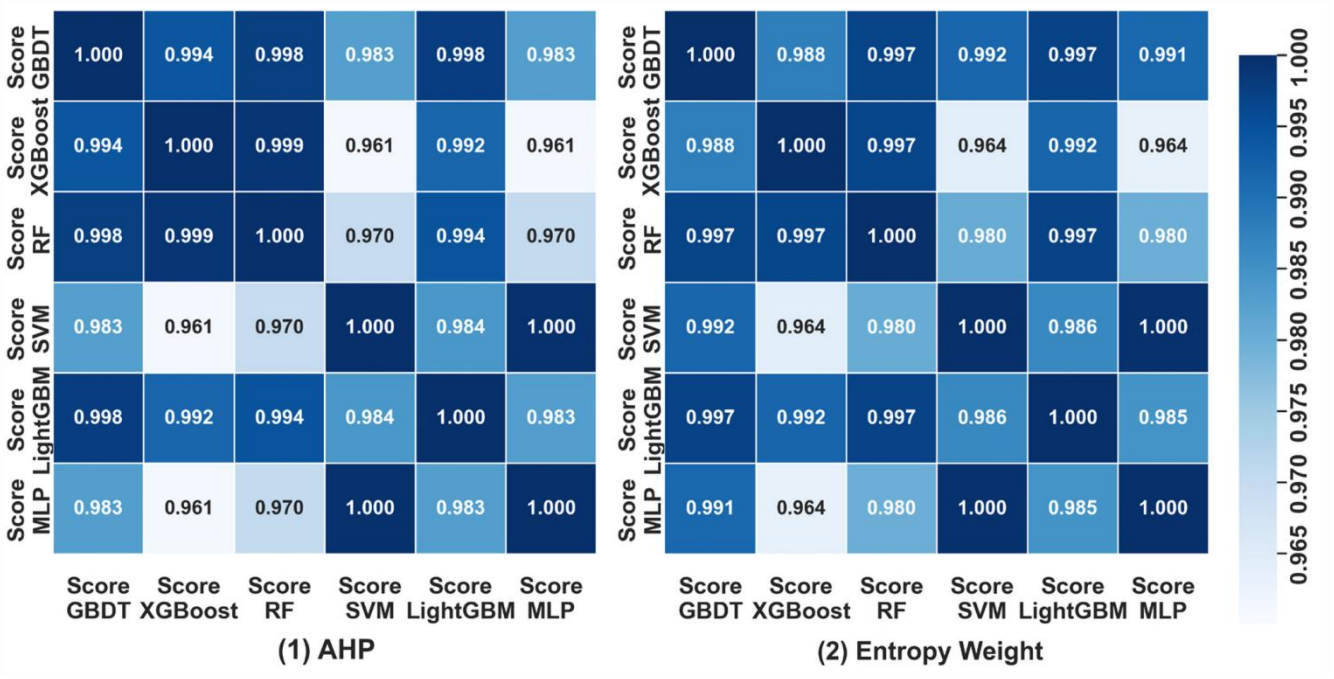

Figure 3: Correlation matrix of severity rankings across six machine learning models using AHP and Entropy Weight methods, highlighting the average Spearman rank correlation coefficient.

4.1.3 Robustness via ensemble integration

To further mitigate the potential bias of individual models, the final weighting scheme was constructed through ensemble integration. Instead of relying on a single "best" predictor, we aggregated the normalized importance scores from the highly consistent base learners. Feature contribution analysis indicated that tree-based ensemble methods (e.g., Random Forest and LightGBM) provided the most stable weight distributions. By integrating these diverse algorithmic perspectives, the final FSI_{ML} reduces random noise and reflects a consensus structural pattern of urban flood severity.

4.2 Spatial patterns of urban flood disaster severity

The hybrid-weighting models reveal a highly robust and spatially coherent pattern of urban flood severity across the 20 representative cities. A pronounced north–south gradient emerges, accompanied by clear city-type patterns shaped by hydrometeorological forcing, exposure characteristics, and urban morphological conditions.

4.2.1 North–south differentiation in severity levels

Both weighting schemes consistently indicate that southern riverine and coastal cities experience significantly higher flood severity than northern cities. Wuhan, Guangzhou, Shenzhen, Hangzhou, and Chengdu exhibit persistently elevated severity

https://doi.org/10.5194/egusphere-2026-2501
Preprint. Discussion started: 22 May 2026

levels, with most events categorized as high or very high. These cities are influenced by intense monsoonal rainfall, dense river networks, and, in coastal areas, typhoon-induced storm surges, creating multiple pathways for high-impact flooding (Fig. 4).

In contrast, northern cities such as Shenyang, Tianjin, Yantai, and Dalian are dominated by very low- and low-severity events. Flooding in these cities is typically limited to short-duration waterlogging with modest socioeconomic impacts. Although occasional severe events occur in individual years, the long-term distribution remains skewed toward low and moderate severity.

This sharp differentiation demonstrates that southern cities face a chronic high-severity regime, whereas northern cities experience primarily localized, episodic, and lower-intensity flood disturbances.

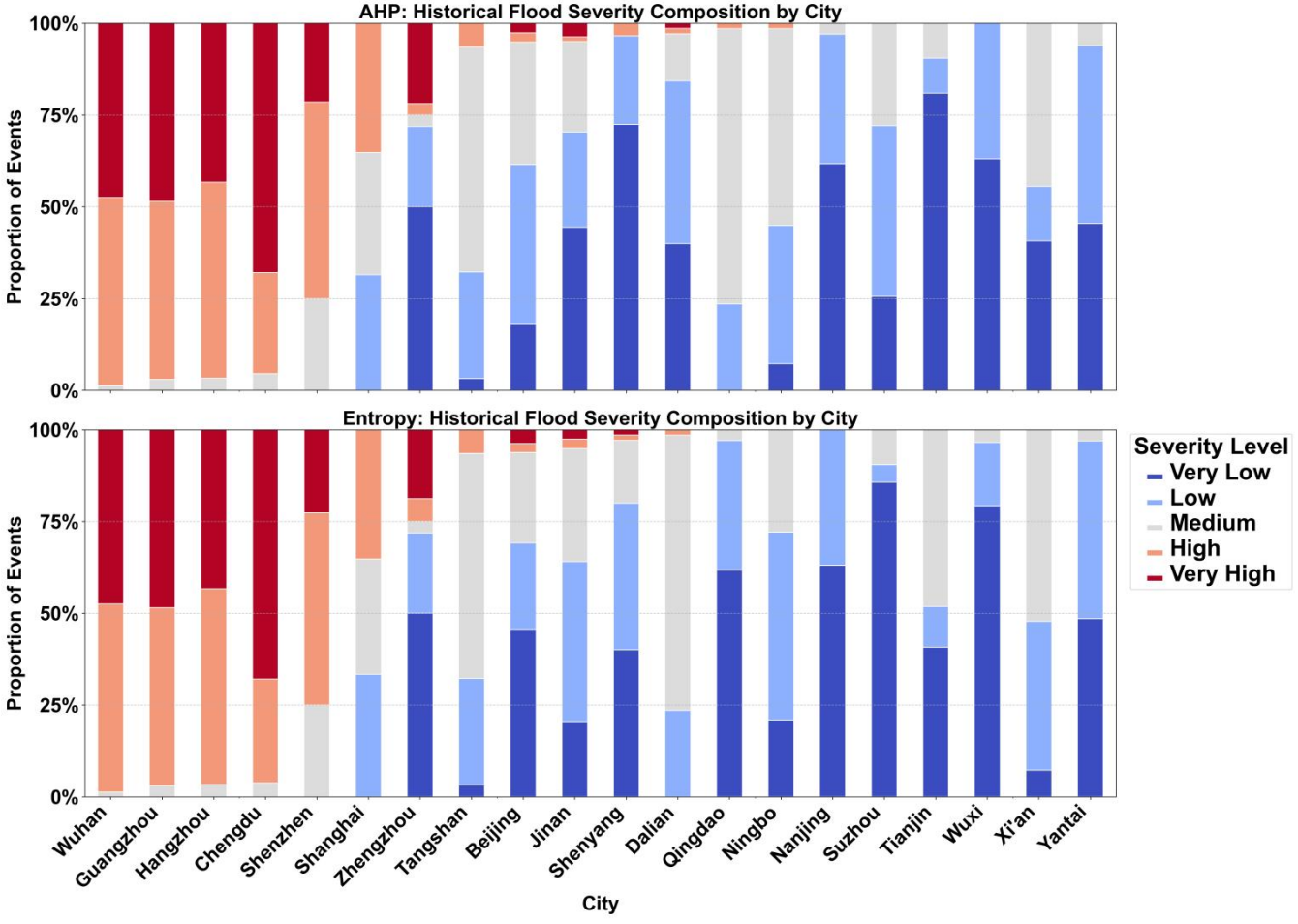

Figure 4: Comparison of the composition of historical flood severity in various cities based on AHP and the entropy weight method.

https://doi.org/10.5194/egusphere-2026-2501
Preprint. Discussion started: 22 May 2026

4.2.2 City-level ranking and typological characteristics

A combined assessment using average severity levels and the proportion of high-severity events provides a clear ranking of flood-prone cities and reveals three distinct city types.

According to the ranking results, major southern cities such as Wuhan, Guangzhou, Shenzhen, Hangzhou, and Chengdu occupy the highest positions, with average severity levels exceeding 3 and high-severity events accounting for nearly all recorded cases. These cities are typically located along major rivers, coastal zones, or densely connected river networks, and are exposed to compound flood risks driven by intense rainfall, typhoon-induced storm surges, and elevated river levels. Such conditions contribute to their high exposure and vulnerability, making them the core hotspots of urban flood risk in China. In these cities, high-severity events are not only frequent but also remain persistently elevated over time, further confirming the "strong-in-the-south" spatial pattern identified in earlier sections (Fig. 5).

In contrast, northern cities such as Shenyang, Tianjin, and Qingdao rank substantially lower, with average severity levels generally below 1.5 and a markedly low proportion of high-severity events. Most flood events in these locations manifest as localized waterlogging or short-duration inundation, reflecting predominantly low-to-moderate severity. Although occasional extreme events occur in specific years, the long-term structure of flood risk in northern cities remains relatively mild, displaying a pattern of "low and stable" severity (Fig. 5).

Notably, several central coastal and riverine cities—such as Shanghai and Ningbo—exhibit multiple coexisting severity levels, with all five categories (very low, low, medium, high, and very high) represented to varying extents. These cities lie at the interface of complex hydrological systems and densely developed urban spaces. They are susceptible both to pluvial flooding triggered by intense rainfall and to high-impact inundation associated with astronomical tides or abrupt rises in water levels. Their mid-to-high ranking reflects a complex and uncertain flood-risk structure shaped by the combined influence of hydrometeorological and urban-system factors (Fig. 5).

https://doi.org/10.5194/egusphere-2026-2501
Preprint. Discussion started: 22 May 2026

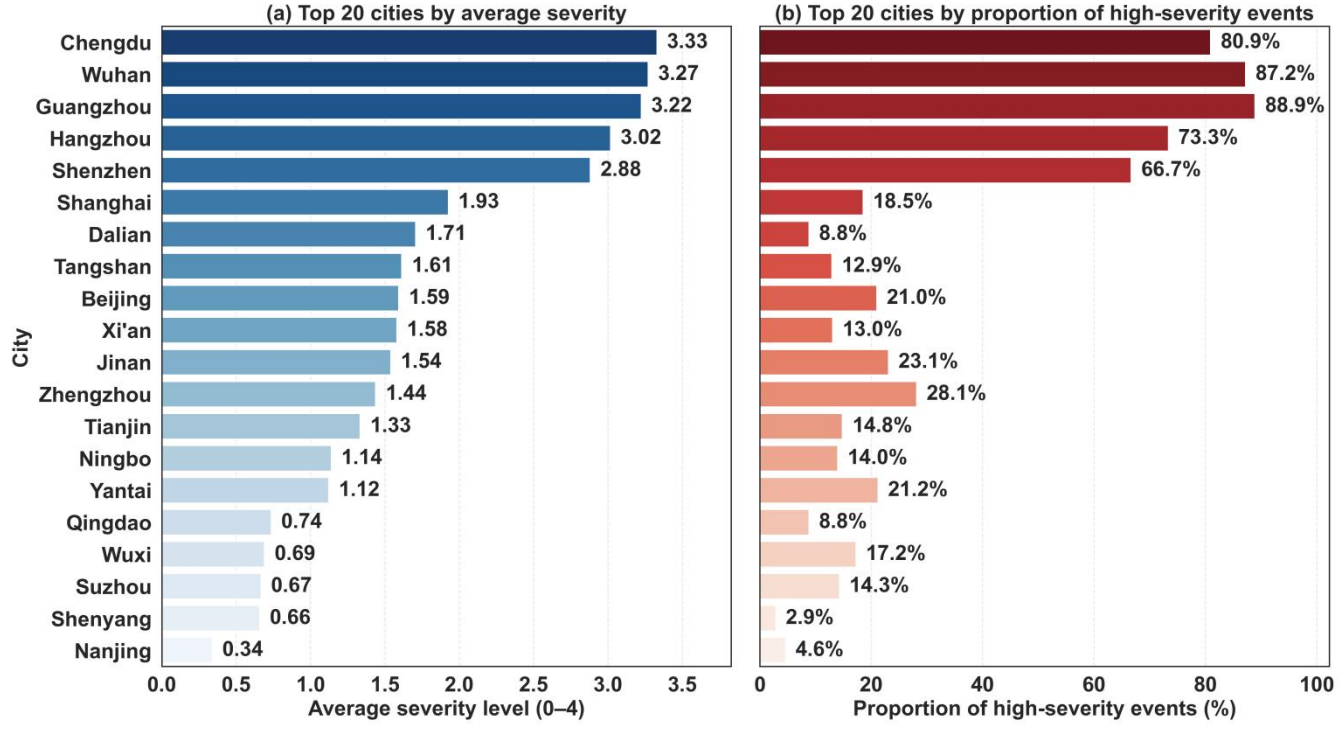

Figure 5: (a) Top 20 cities by average severity level and (b) Top 20 cities by proportion of high-severity events.

Taken together, the spatial ranking illustrates a stratified urban flood-risk landscape in China, with persistent southern hotspots, stable northern low-risk zones, and mixed-pattern coastal megacities. Synthesizing the above results, three robust spatial findings emerge: (A) a pronounced "strong-south, weak-north" gradient in urban flood severity, with southern riverine and coastal cities forming persistent high-severity hotspots; (B) the existence of a stable low-severity regime in most northern cities, punctuated by only a small share of high-impact events; and (C) the presence of mixed-pattern coastal megacities (e.g., Shanghai, Ningbo) that exhibit diversified severity structures and compound hazard mechanisms. These three city types provide a structural lens for interpreting subsequent temporal trajectories and driving-factor differences.

4.3 Temporal evolution and regional characteristics of flood disaster severity

The comparative analysis of AHP- and entropy-weighted models indicates that urban flood severity from 2000 to 2024 has evolved through three distinct phases: a period of volatility (2000–2010), a transitional phase of adjustment (2010–2020), and a recent phase of moderation (2021–2024). Early volatility was driven by the mismatch between rapid urbanization and drainage capacity, resulting in frequent events. Post-2010, while infrastructure improvements like sponge-city projects significantly curbed medium- and low-severity events, the models highlight that very-high-severity events did not decline linearly, instead manifesting as sporadic surges in years such as 2016 and 2021 (Fig. 6).

https://doi.org/10.5194/egusphere-2026-2501
Preprint. Discussion started: 22 May 2026

This temporal nonlinearity is closely associated with widening regional disparities. Southern cities generally maintain a persistent high-exposure regime with average severity levels of 3–4 due to monsoonal factors, whereas northern cities exhibit a stable low-severity baseline punctuated by rare but intense extremes. The 2021 spike exemplifies this divergence, as northern cities like Zhengzhou experienced unprecedented abrupt shifts from low to extreme severity. However, the generalized decline in severity since 2022 suggests that upgraded emergency protocols are gradually mitigating risks across both high-exposure southern zones and northern regions prone to episodic extremes.

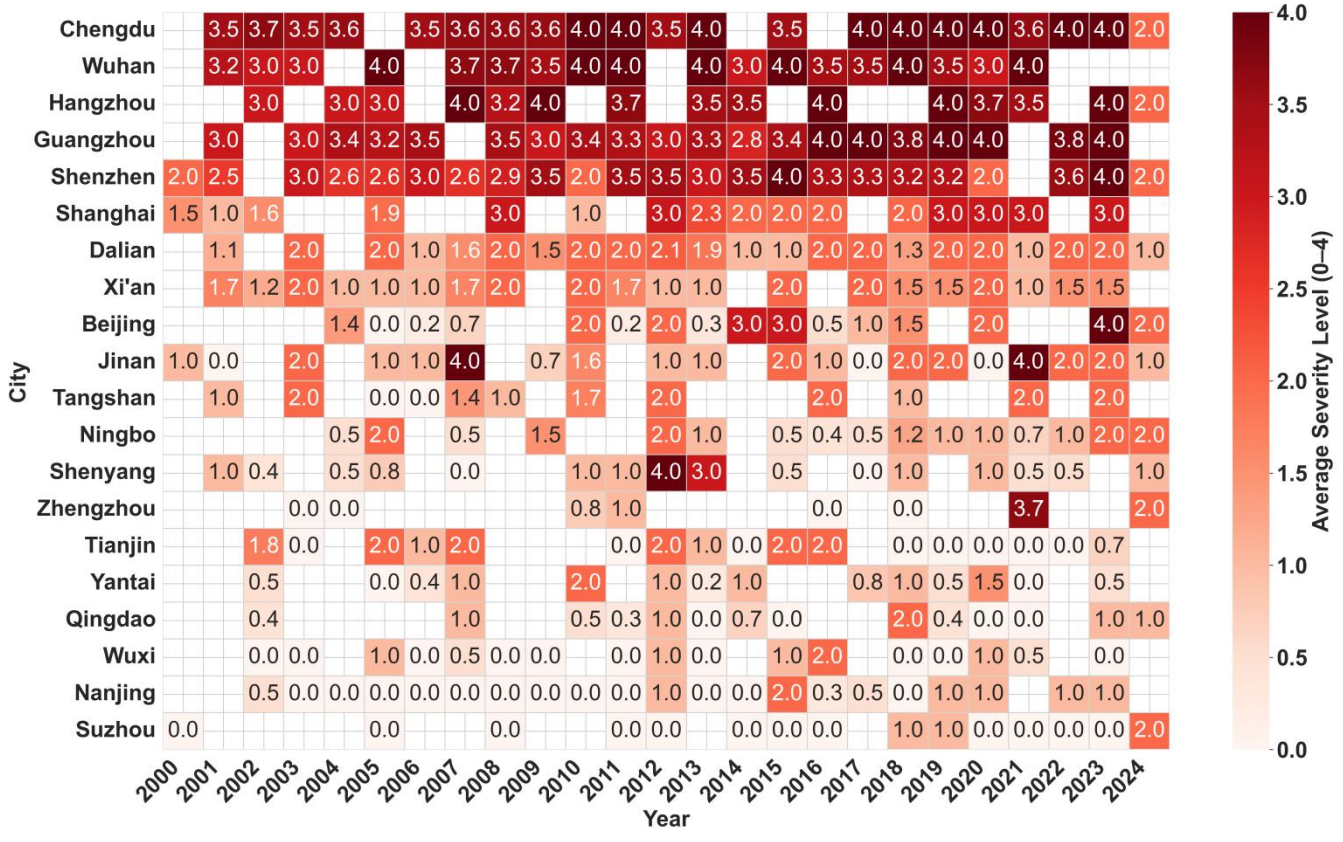

Figure 6: Heatmap of the average flood severity levels across 20 cities from 2000 to 2024.

4.4 Urban-scale severity trends and risk differentiation

Trend-line analysis of annual average flood severity provides a refined perspective on the long-term trajectories of urban flood risk across the 20 cities. By examining both the direction and distribution of event severity over time, this section reveals how cities are diverging into distinct evolutionary pathways shaped by hydrometeorological exposure, urbanization intensity, and systemic drainage capacity.

https://doi.org/10.5194/egusphere-2026-2501
Preprint. Discussion started: 22 May 2026

4.4.1 Long-term trajectories of severity growth or mitigation

In southern cities, trend lines for Wuhan, Guangzhou, Shenzhen, and Hangzhou exhibit a sustained upward or persistently high trajectory, with most annual data points clustering within medium-to-high severity ranges. This suggests that these cities have entered a prolonged high-severity stage in which both flood frequency and impact remain elevated. The concentration of the concentration of high-severity points across most years indicates that the interplay of high-intensity rainfall, expanding impervious surfaces, and complex hydrological settings continues to reinforce their vulnerability. In these cities, even years with relatively lower rainfall show limited relief, reflecting a structural exposure pattern that has become embedded in the urban system (Fig. 7).

Other southern cities, such as Chengdu, display upward trajectories that are more gradual but similarly persistent. The persistence of mid-to-high severity events suggests that although local improvements in drainage and early-warning systems may reduce some impacts, the cumulative effects of concentrated monsoon rainfall and basin-scale hydrodynamics continue to shape their long-term risk profile.

https://doi.org/10.5194/egusphere-2026-2501
Preprint. Discussion started: 22 May 2026

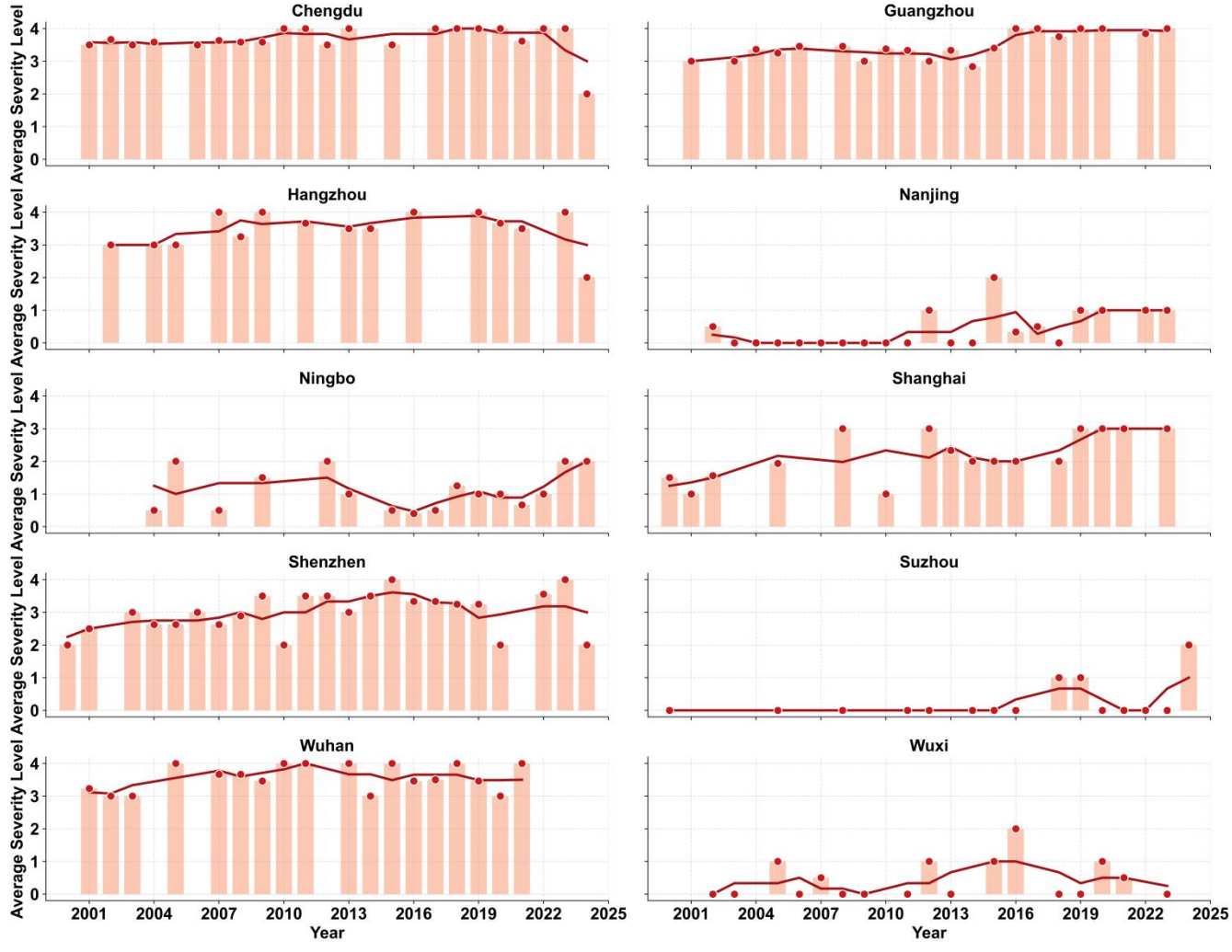

Figure 7: Temporal Evolution of Flood Severity in Southern Cities from 2000 to 2024.

4.4.2 Stabilizing or declining trends in lower-risk northern cities

In northern cities, the trend lines for Qingdao, Dalian, and Yantai exhibit relatively flat or mildly declining slopes, with scatter points concentrated within low-severity categories. This indicates that long-term flood risk has remained largely stable and, in some cases, marginally improved. Continuous drainage-network upgrading, combined with lower precipitation forcing and slower rates of impervious-surface expansion compared with southern megacities, has helped maintain a steady or slightly declining risk trajectory. The consistency of low-severity outcomes across years shows that while minor waterlogging remains common, it rarely escalates into high-impact events (Fig. 8).

https://doi.org/10.5194/egusphere-2026-2501
Preprint. Discussion started: 22 May 2026

320 However, these stabilizing patterns do not imply immunity to extreme rainfall. Cities such as Shenyang and Tianjin predominantly fall within low-severity but still exhibit occasional moderate spikes, suggesting that localized convective storms can temporarily disrupt otherwise stable risk trajectories.

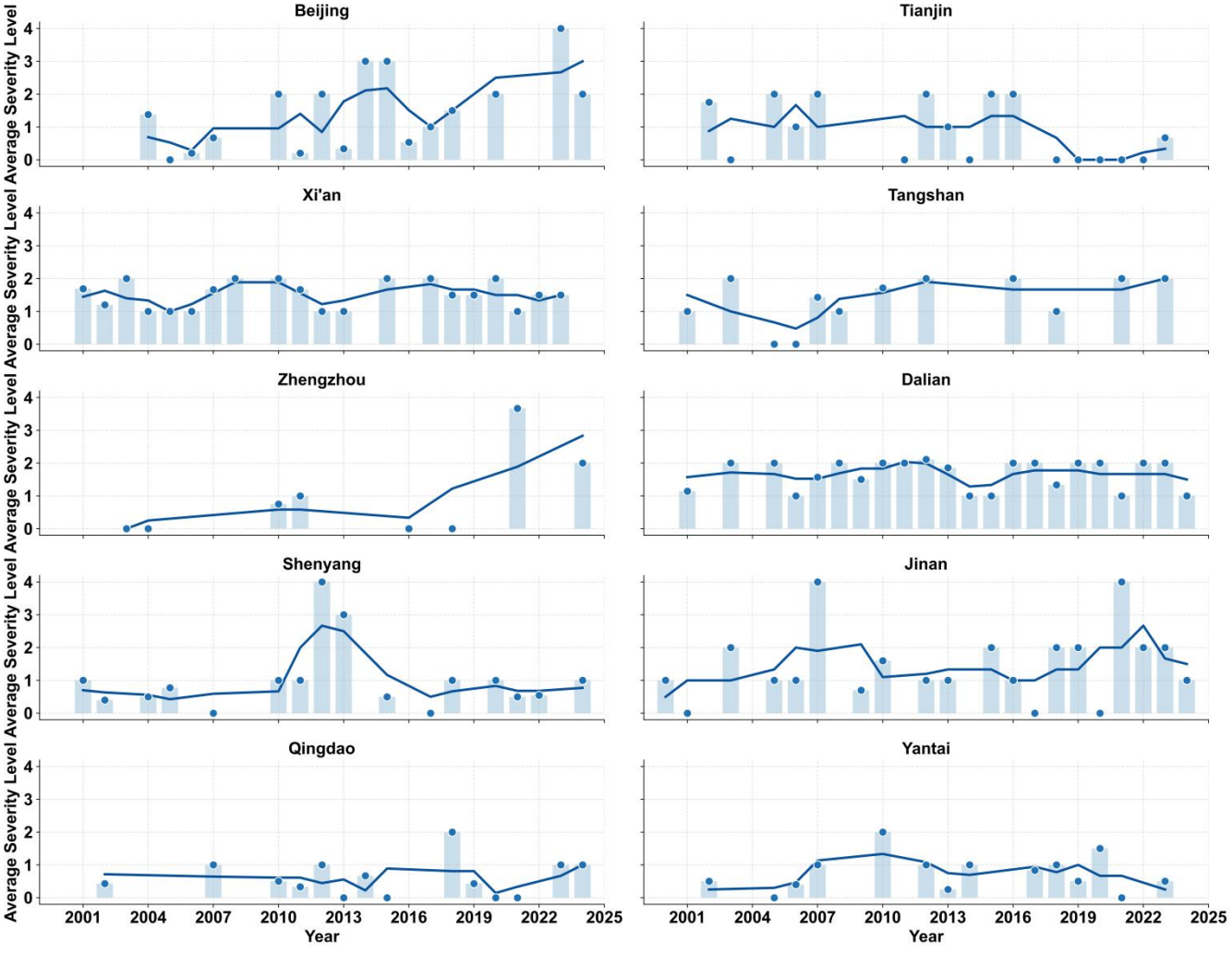

Figure 8: Temporal Evolution of Flood Severity in Northern Cities from 2000 to 2024.

325 **4.4.3 Cities exhibiting upward trajectories and episodic extremes**

A separate group of cities, including Beijing and Zhengzhou, demonstrates upward trends punctuated by abrupt, high-severity spikes. In these cases, the majority of scatter points fall within low or moderate categories, yet severe upward deviations occur in years dominated by extreme rainfall anomalies. The trend lines for these cities thus represent an emerging hybrid risk regime: overall low baseline severity, but rising sensitivity to exceptionally high-intensity precipitation.

https://doi.org/10.5194/egusphere-2026-2501
Preprint. Discussion started: 22 May 2026

Zhengzhou's pronounced spike in 2021 illustrates how short-duration, record-breaking storms can expose latent weaknesses in drainage design standards and emergency-response capacity. Similarly, Beijing has experienced occasional upward deviations linked to storm events that exceed historical norms. These episodic extremes indicate that, unlike southern cities where high severity is persistent, northern high-impact events are more contingent on rare but increasingly plausible meteorological conditions under a warming climate.

4.5 SHAP analysis results for the hybrid-weighted model

To further illuminate the mechanisms underlying the hybrid-weighted models and to understand how individual variables contribute to flood severity estimation, SHAP analysis was applied to the AHP- and entropy-based hybrid frameworks. The results provide insight into how exposure, socioeconomic losses, and public attention interact within the machine-learning models, and reveal distinct interpretive patterns shaped by subjective and objective weighting philosophies.

4.5.1 Feature contribution analysis of the AHP hybrid model

In the AHP hybrid model, affected area shows the highest mean absolute SHAP value, indicating that spatial exposure is the primary determinant of severity. Affected population also contributes strongly and positively, reflecting its direct relationship with potential disaster scale. Online public attention provides moderate supplementary value, capturing public-perception signals during high-impact events. Economic losses and fatalities contribute less, consistent with the expert-driven weighting scheme that distributes importance more evenly across indicators (Fig. 9). Overall, the AHP model presents a balanced interpretive structure centered on physical and demographic exposure.

4.5.2 Feature contribution analysis of the entropy-weighted hybrid model

The entropy-weighted hybrid model retains affected area as the top contributor but shows markedly higher and more stable SHAP values for economic losses. This reflects the entropy method's sensitivity to indicators with high variability and its tendency to amplify objective dispersion within the dataset. Affected population remains influential, while fatalities and online popularity show weaker contributions due to their limited variance (Fig. 9). The entropy model therefore emphasizes physical and economic exposure more strongly than social-perception indicators.

4.5.3 Comparative of interpretive patterns and implications for severity Modeling

A comparison of the SHAP results from the AHP-based and entropy-based hybrid models reveals several key differences in their interpretive structures: (1) In the AHP hybrid model, exposure-related variables such as affected area and population make prominent contributions, but the overall weighting remains more balanced, reinforcing model interpretability and coordination across multiple indicators; (2) The entropy-based hybrid model demonstrates higher sensitivity to economic losses, reflecting the greater influence of data-driven variability and emphasizing the quantitative representation of disaster intensity and exposure; (3) The AHP model may offer greater interpretability when addressing regional heterogeneity and

https://doi.org/10.5194/egusphere-2026-2501
Preprint. Discussion started: 22 May 2026

360 extreme events, whereas the entropy model is better suited for capturing long-term trends and broader shifts in severity classification.

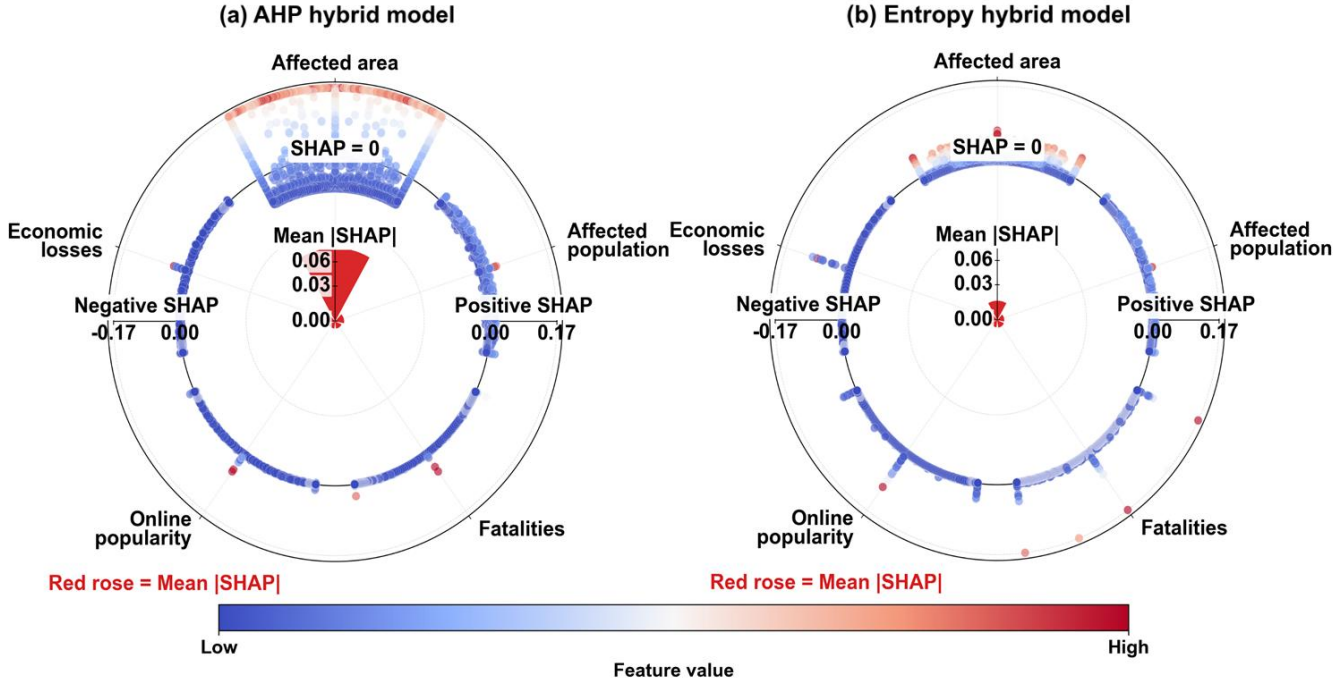

Figure 9: SHAP Feature Importance Results of the Hybrid Machine Learning Model.

5 Discussion

365 This study draws on long-term disaster time-series data from 20 cities to uncover pronounced spatial patterns, temporal dynamics, and underlying mechanisms of urban flood disasters in China. These variations arise from the combined influences of natural environmental conditions, socio-economic structures, urbanization trajectories, and urban morphological characteristics, reflecting a typical coupled "nature–society–urban system" framework (Wu et al., 2021).

First, the formation of urban flooding is shaped by a multifactorial and highly interactive mechanism. Climatic regimes, the 370 timing of monsoon or flood seasons, topographic variation, and the density of river networks collectively determine the dominant rainfall regimes and the fundamental patterns of runoff generation (Wu et al., 2020). In southern China, the subtropical monsoon produces frequent and intense rainstorms, and the combination of dense river networks and low-lying terrain amplifies the occurrence of compound hazards involving regional rainstorms, urban waterlogging, and fluvial flooding (Wang, Y. et al., 2022). In contrast, rainfall intensity is generally weaker in northern cities, where urban flooding is 375 primarily attributed to localized cloudbursts and drainage-system bottlenecks, resulting in flood-generation mechanisms that differ substantially from those in the south (Ali et al., 2025). The interaction between natural hydrometeorological processes

https://doi.org/10.5194/egusphere-2026-2501
Preprint. Discussion started: 22 May 2026

and socio-urban systems thus gives rise to a pronounced north–south differentiation in flood-disaster characteristics at a large spatial scale (Song et al., 2024).

Second, regional disparities reflect the influence of divergent urbanization trajectories and spatial development patterns. The results indicate that cities such as Wuhan, Guangzhou, Chengdu, and Shenzhen exhibit very high proportions of high-severity flood events, driven not only by intense precipitation but also by rapid urban expansion, the continued expansion of impervious surfaces, and the increasing burden on aging drainage infrastructure in older urban districts (Chen et al., 2025). By comparison, although northern cities such as Qingdao, Shenyang, and Tianjin have also undergone substantial urbanization, their weaker precipitation forcing and recent upgrades to drainage systems have contributed to stable or declining flood severity. Cities such as Shanghai and Ningbo exhibit multiple coexisting severity levels, reflecting complex hazard mechanisms shaped by tidal backwater influences, low-lying terrain, dense channel networks, and the morphological configuration of megacities.

Third, although the multi-source datasets used in this study improve the spatiotemporal representation of flood events, data acquisition remains a major challenge. Social media data provide timely updates, but they are spatially biased toward densely populated and digitally active areas, which may lead to underrepresentation of events in less populated regions. News reports are relatively more objective, yet they often suffer from reporting delays and uneven spatial coverage. In addition, historical flood information is frequently incomplete, and missing observations may need to be interpolated, introducing further uncertainty. These issues make it difficult to construct a consistent, comparable, and high-quality urban flood database across cities and over time. Future studies should therefore prioritize more standardized data-collection frameworks and explicitly assess the influence of data uncertainty on model outcomes.

Finally, the long-term evolution trajectories and city-type differences identified in this study offer important implications for understanding urban flood risk management in China. The results indicate that flood management priorities differ across city types because of variations in rainfall regimes, hydrological settings, and urban infrastructure conditions. For southern cities, such as Wuhan, Guangzhou, and Shenzhen, where intense precipitation and dense river networks are more common, approaches such as green infrastructure, sponge city development, and improved drainage systems may be especially relevant (Kong et al., 2021). For northern cities, such as Tianjin, Shenyang, and Qingdao, although flood occurrence is generally less frequent, extreme events in several major cities, such as Beijing and Zhengzhou, reveal persistent weaknesses in drainage systems and vulnerable functional zones, suggesting the need for targeted improvements in stormwater management, monitoring, and emergency preparedness (Ghosh et al., 2021). Overall, these findings highlight the importance of moving from isolated engineering responses toward a more integrated and resilience-based perspective on urban flood management.

Future research should therefore focus on three directions. One is to construct more comprehensive geospatial big-data infrastructures for urban flooding by integrating high-resolution remote sensing, crowdsourced observations, and smart-sensor networks, together with explicit uncertainty quantification of data gaps and interpolation schemes. A second priority is to couple the data-driven severity models with process-based hydrological and hydrodynamic simulations, enabling

https://doi.org/10.5194/egusphere-2026-2501
Preprint. Discussion started: 22 May 2026

scenario analysis under projected climate and urbanization pathways. Third, extending the analytical scale from city-wide averages to intra-urban functional zones and critical infrastructures would allow a more refined assessment of exposure, vulnerability and resilience, and provide more actionable guidance for targeted adaptation and resilience planning.

6 Conclusion

This study integrates multi-source urban flood disaster data from 2000 to 2024 and develops an urban flood-severity assessment framework using hybrid weighting and machine-learning models. Through spatial and temporal analyses, it systematically reveals the evolutionary characteristics of flood disasters across representative Chinese cities. The main conclusions are as follows:

(1) Urban flood disasters in China exhibit a clear north-south divide. Southern cities, with high-intensity monsoon rainfall, dense river networks, and low-lying terrain, experience consistently high flood severity and frequent events. In contrast, northern cities, while facing lower overall risk, display distinct high-intensity flood characteristics during extreme-event years, highlighting vulnerabilities in urban systems exacerbated by rapid urbanization and climate change.

(2) The structural composition of flood disasters varies significantly across cities. Cities such as Wuhan, Guangzhou, and Shenzhen consistently experience high severity, while cities such as Shanghai and Ningbo display a mix of flood severity levels. In contrast, cities such as Tianjin and Shenyang are primarily affected by localized, low-intensity flooding, and their flood severity evolution is strongly influenced by urban morphology and drainage infrastructure.

(3) Long-term trends in urban flood severity show a pattern of “an overall increasing trend with localized intensification”. Southern cities display a rising risk trajectory, whereas northern cities remain relatively stable; however, extreme events highlight latent vulnerabilities within northern urban systems, reflecting the joint influence of climate change and rapid urban expansion.

(4) Southern cities need basin-scale resilience strategies, while northern cities should enhance infrastructure for extreme events. Urban flood management in China should shift toward integrated resilience strategies. Future research should focus on improving data systems, strengthening hydrological models, and advancing risk assessment at the level of urban functional zones.

Code and data availability

The source code developed for this study will be made publicly available on GitHub upon publication at: https://github.com/jingyu-sun-yw/FloodFusion-Ensemble. The DEM data were obtained from the Copernicus DEM GLO-30 dataset on the Google Earth Engine platform (https://earthengine.google.com/), with the dataset ID COPERNICUS/DEM/GLO30 and a spatial resolution of approximately 30 m. This dataset is a digital surface model (DSM), which includes the height information of surface features such as buildings and vegetation. The administrative boundary data

https://doi.org/10.5194/egusphere-2026-2501
Preprint. Discussion started: 22 May 2026

were derived from Tianditu, the National Platform for Common Geospatial Information Services of China. The datasets used to generate the figures in this study are available in the GitHub repository: https://github.com/jingyu-sun-yw/FloodFusion-Ensemble. Other data generated or analyzed during this study are available from the corresponding author upon reasonable request.

Author contributions

GP: Writing – review & editing, Methodology, Conceptualization, Funding acquisition. YS: Writing – original draft, Visualization, Methodology, Formal analysis, Data curation. MW: Methodology, Data curation. MC: Writing – review & editing, Supervision, Conceptualization. FZ: Writing – review & editing, Methodology.

Competing interests

The authors declare no competing interests.

Disclaimer

Publisher's note: Copernicus Publications remains neutral with regard to jurisdictional claims made in the text, published maps, institutional affiliations, or any other geographical representation in this paper. While Copernicus Publications makes every effort to include appropriate place names, the final responsibility lies with the authors.

Acknowledgements

We thank editor and reviewers for helping us improving the clarity of the paper.

Financial support

This research was funded by the National Natural Science Foundation of China (grant number 42201517)

References

Ahmad, I., Ping, W., Ullah, S., Faqeih, K.Y., Alamri, S.M., Alamery, E.R., Abalkhail, A.A.A. and Bilal Jan, H.M.: Spatiotemporal Mapping of Urban Flood Susceptibility: A Multi-Criteria GIS-Based Assessment in Nangarhar, Afghanistan. Land, 14, 2376. https://doi.org/10.3390/land14122376, 2025.

https://doi.org/10.5194/egusphere-2026-2501
Preprint. Discussion started: 22 May 2026

Ali, Y., Afnan, J., Jannat, M., and Uddin, M. M.: Assessing alteration of urban floodplains using remote sensing and GIS: a three decade analysis (1992–2022). Geol. Ecol. Landsc., 1–16. https://doi.org/10.1080/24749508.2025.2524209, 2025.

Bagheri, A. and Liu, G.-J.: Climate change and urban flooding: assessing remote sensing data and flood modeling techniques: a comprehensive review. Environ. Rev., 33, 1–14. https://doi.org/10.1139/er-2024-0065, 2025.

Ban, J., Sutton, C., Ma, Y. Lin, C., and Chen, K.: Association of flooding exposure with cause-specific mortality in North Carolina, United States. Nat. Water, 1, 1027–1034. https://doi.org/10.1038/s44221-023-00167-5, 2023.

Bhusal, A., Thakur, B., Kalra, A., Benjankar, R., and Shrestha, A.: Evaluating the Effectiveness of Best Management Practices in Adapting the Impacts of Climate Change-Induced Urban Flooding. Atmosphere, 15, 281. https://doi.org/10.3390/atmos15030281, 2024.

Cao, W., Zhou, Y., Güneralp, B., Li, X., Zhao, K., and Zhang, H.: Increasing global urban exposure to flooding: An analysis of long-term annual dynamics. Sci. Total Environ., 817, 153012. https://doi.org/10.1016/j.scitotenv.2022.153012, 2022.

Chen, J., Li, Y., Zhang, L., and Tian, Y.: Impact of Interactions between Different Rainfall Patterns and River Water Levels on Urban Flooding in Inland Plain Cities. Water Resour. Manag., 39, 7515–7539. https://doi.org/10.1007/s11269-025-04306-3, 2025.

Chen, J., Gao, C., Zhou, H., Wang, Q., She, L., Qing, D., and Cao, C.: Urban Flood Risk Assessment Based on a Combination of Subjective and Objective Multi-Weight Methods. Appl. Sci., 14, 3694. https://doi.org/10.3390/app14093694, 2024.

Dai, D., Bo, M., Ren, X., and Dai, K.: Application and exploration of artificial intelligence technology in urban ecosystem-based disaster risk reduction: A scoping review. Ecol. Indic., 158, 111565. https://doi.org/10.1016/j.ecolind.2024.111565, 2024.

Duan, C., Zheng, X., Li, R., and Wu, Z.: Urban flood vulnerability Knowledge-Graph based on remote sensing and textual bimodal data fusion. J. Hydrol., 633, 131010. https://doi.org/10.1016/j.jhydrol.2024.131010, 2024.

Fang, D., Xu, F., Jin, X., Song, C., Gao, P., Sun, L., Wang, D., and Feng, K.: Stress-testing the cascading economic impacts of urban flooding across 306 Chinese cities. Nat. Cities 3, 89–101. https://doi.org/10.1038/s44284-025-00372-1, 2026.

Fu, S., Schultz, D. M., Lyu, H., Zheng, Z., and Zhang, C., 2025. Creating a national urban flood dataset for China from news texts (2000–2022) at the county level. Hydrol. Earth Syst. Sci., 29, 767–783. https://doi.org/10.5194/hess-29-767-2025, 2025.

Ge, H. and Zhu, L.: Extreme flood levels during the operation of cascade reservoirs: A case study of the Lower Yangtze River in 2020. Water, 15, 851. https://doi.org/10.3390/w15050851, 2023.

Ghosh, P., Sudarsan, J.S., and Nithiyanantham, S.: Nature-Based Disaster Risk Reduction of Floods in Urban Areas. Water Resour. Manag., 38, 1847–1866. https://doi.org/10.1007/s11269-024-03757-4, 2024.

Guo, K., Guan, M., and Yu, D.: Urban surface water flood modelling – a comprehensive review of current models and future challenges. Hydrol. Earth Syst. Sci., 25, 2843–2860. https://doi.org/10.5194/hess-25-2843-2021, 2021.

Hu, Y., Connor, D. S., Stuhlmacher, M., Peng, J., and Turner, B. L.II.: More urbanization, more polarization: evidence from two decades of urban expansion in China. npj Urban Sustain., 4, 33. https://doi.org/10.1038/s42949-024-00170-z, 2024.

https://doi.org/10.5194/egusphere-2026-2501
Preprint. Discussion started: 22 May 2026

Hussain, M., Tayyab, M., Ullah, K., Ullah, S., Rahman, Z. U., Zhang, J., and Al-Shaibah, B.: Development of a new integrated flood resilience model using machine learning with GIS-based multi-criteria decision analysis. Urban Clim., 50, 101589. https://doi.org/10.1016/j.uclim.2023.101589, 2023.

Jiang, Y., Zevenbergen, C., and Ma, Y.: Urban pluvial flooding and stormwater management: A contemporary review of China's challenges and "sponge cities" strategy. Environ. Sci. Policy, 80, 132–143. https://doi.org/10.1016/j.envsci.2017.11.016, 2018.

Kong, F., Sun, S., and Wang, Y.: Comprehensive understanding the disaster-causing mechanism, governance dilemma and targeted countermeasures of urban pluvial flooding in china. Water, 13, 1762. https://doi.org/10.3390/w13131762, 2021.

Li, C., Sun, N., Lu, Y., Guo, B., Wang, Y., Sun, X., and Yao, Y.: Review on Urban Flood Risk Assessment. Sustainability, 15, 765. https://doi.org/10.3390/su15010765, 2023.

Li, G., Liu, J., and Shao, W.: Urban flood risk assessment under rapid urbanization in Zhengzhou City, China. Reg. Sustain., 4, 332–348. https://doi.org/10.1016/j.regsus.2023.08.004, 2023.

Li, Y., Wang, L., Li, F., Peng, S.G., and Ding, C.: Quantitative estimation of urban flood damage from storm surges for a coastal city. Nat. Hazards, 121, 16915–16934. https://doi.org/10.1007/s11069-025-07456-0, 2025.

Liang, P. and Ding, Y.: The long-term variation of extreme heavy precipitation and its link to urbanization effects in Shanghai during 1916–2014. Adv. Atmos. Sci., 34, 321–334. https://doi.org/10.1007/s00376-016-6120-0, 2017.

Liu, X., Zhou, P., Lin, Y., Sun, S., Zhang, H., Xu, W., and Yang, S.: Influencing Factors and Risk Assessment of Precipitation-Induced Flooding in Zhengzhou, China, Based on Random Forest and XGBoost Algorithms. Int. J. Environ. Res. Public Health, 19, 16544. https://doi.org/10.3390/ijerph192416544, 2022.

Luo, Y., Zhang, J., Yu, M., Liang, X., Xia, R., Gao, Y., Gao, X., and Yin, J.: On the influences of urbanization on the extreme rainfall over Zhengzhou on 20 July 2021: A convection-permitting ensemble modeling study. Adv. Atmos. Sci., 40, 393–409. https://doi.org/10.1007/s00376-022-2048-8, 2023.

Misra, A., White, K., Nsutezo, S.F., Straka, W. III., and Lavista, J.: Mapping global floods with 10 years of satellite radar data. Nat. Commun., 16, 5762. https://doi.org/10.1038/s41467-025-60973-1, 2025.

Peng, J. and Zhang, J.: Urban flooding risk assessment based on GIS- game theory combination weight: A case study of Zhengzhou City. Int. J. Disaster Risk Reduct., 77, 103080. https://doi.org/10.1016/j.ijdrr.2022.103080, 2022.

Qi, S., Cao, S., Hu, S., and Liu, Q.: Bibliometric analysis on urban flood and waterlogging disasters during the period of 1998—2022. Nat. Hazards, 120, 12595–12612. https://doi.org/10.1007/s11069-024-06710-1, 2024.

Rentschler, J., Avner, P., Marconcini, M. Su, R., Strano, E., Vousdoukas, M., and Hallegatte, S.: Global evidence of rapid urban growth in flood zones since 1985. Nature, 622, 87–92. https://doi.org/10.1038/s41586-023-06468-9, 2023.

Romali, N.S., Sulong, S., and Kawasaki, A.: A Systematic Review of Flood Damage Assessment: Insight for the Data-Scarce Regions. Water Resour. Manag., 39, 4707–4734. https://doi.org/10.1007/s11269-025-04265-9, 2025.

Rogers, J.S., Maneta, M.P., Sain, S.R. Madaus, L.E., and Hacker, J.P.: The role of climate and population change in global flood exposure and vulnerability. Nat. Commun., 16, 1287. https://doi.org/10.1038/s41467-025-56654-8, 2025.

https://doi.org/10.5194/egusphere-2026-2501
Preprint. Discussion started: 22 May 2026

Sanders, B.F., Schubert, J.E., Kahl, D.T. Mach. K.J., Brady, D., Aghakouchak, A., Forman, F., Matthew, R.A., Ulibarri, N., and Davis, S.J.: Large and inequitable flood risks in Los Angeles, California. Nat. Sustain., 6, 47–57. https://doi.org/10.1038/s41893-022-00977-7, 2023.

Song, X., Xu, N., Zhang, J., and He, R.: Urban flooding in China: current status, causes and challenges. Adv. Water Sci., 35, 357-373. https://doi.org/10.14042/j.cnki.32.1309.2024.03.001, 2024.

Tan, L. and Schultz, D. M.: Damage classification and recovery analysis of the Chongqing, China, floods of August 2020 based on social-media data. J. Clean. Prod., 313, 127882. https://doi.org/10.1016/j.jclepro.2021.127882, 2021.

Tellman, B., Sullivan, J.A., Kuhn, C. Kettner, A.J., Doyle, C.S., Brakenridge, G.R., Erickson, T.A., and Slayback, D.A.: Satellite imaging reveals increased proportion of population exposed to floods. Nature, 596, 80–86. https://doi.org/10.1038/s41586-021-03695-w, 2021.

Wang, H., Meng, Y., Xu, H., Wang, H., Guan, X., Liu, Y., Liu,M., and Wu, Z.: Prediction of flood risk levels of urban flooded points though using machine learning with unbalanced data. J. Hydrol., 630, 130742. https://doi.org/10.1016/j.jhydrol.2024.130742, 2024.

Wang, P., Zhu, Y., and Yu, P.: Assessment of Urban Flood Vulnerability Using the Integrated Framework and Process Analysis: A Case from Nanjing, China. Int. J. Environ. Res. Public Health, 19, 16595. https://doi.org/10.3390/ijerph192416595, 2022.

Wang, Y., Li, C., Liu, M., Cui, Q., Wang, H., Lv, J., Li, B., Xiong, Z., and Hu, Y.: Spatial characteristics and driving factors of urban flooding in chinese megacities. J. Hydrol. 613(Pt.B), 128464. https://doi.org/10.1016/j.jhydrol.2022.128464, 2022.

Wing, O.E.J., Pinter, N., Bates, P.D., and Kousky, C.: New insights into US flood vulnerability revealed from flood insurance big data. Nat. Commun., 11, 1444. https://doi.org/10.1038/s41467-020-15264-2, 2020.

Wu, M., Wu, Z., Ge, W., Wang, H., Shen, Y., and Jiang, M.: Identification of sensitivity indicators of urban rainstorm flood disasters: A case study in China. J. Hydrol., 599, 126393. https://doi.org/10.1016/j.jhydrol.2021.126393, 2021.

Wu, Z., Shen, Y., Wang, H., and Wu, M.: An ontology-based framework for heterogeneous data management and its application for urban flood disasters. Earth Sci. Inform., 13, 377–390. https://doi.org/10.1007/s12145-019-00439-3, 2020.

Xu, T., Xie, Z., Jiang, F., Yang, S., Deng, Z., Zhao, L., Wen, G., and Du, Q.: Urban flooding resilience evaluation with coupled rainfall and flooding models: a small area in Kunming City, China as an example. Water Sci. Technol., 87, 2820–2839. https://doi.org/10.2166/wst.2023.149, 2023.

Xu, T., Li, E., Samat, A., Wang, S., and Yu, M.: Evaluation of urban flood-prone regions in Chinese cities based on potential flood hazard assessment model. Nat. Hazards, 121, 18743–18763. https://doi.org/10.1007/s11069-025-07536-1, 2025.

Yang, L., Li, J., Kang, A., Li, S., and Feng, P.: The Effect of Nonstationarity in Rainfall on Urban Flooding Based on Coupling SWMM and MIKE21. Water Resour. Manag., 34, 1535–1551. https://doi.org/10.1007/s11269-020-02522-7, 2020.

Yang, W., Zheng, C., Jiang, X., Wang, H., Lian, J., Hu, D., and Zheng, A.: Study on urban flood simulation based on a novel model of SWTM coupling D8 flow direction and backflow effect. J. Hydrol., 621, 129608. https://doi.org/10.1016/j.jhydrol.2023.129608, 2023.

https://doi.org/10.5194/egusphere-2026-2501
Preprint. Discussion started: 22 May 2026

Yin, D., Chen, Y., Jia, H., Wang, Q., Chen, Z., Xu, C., Li, Q., Wang, W., Yang, Y., Fu, G., and Chen, A. S.: Sponge city practice in China: A review of construction, assessment, operational and maintenance. J. Clean. Prod., 280, 124963. https://doi.org/10.1016/j.jclepro.2020.124963, 2021.

Yin, J., Yu, D., Yin, Z., Liu, M., and He, Q.: Evaluating the impact and risk of pluvial flash flood on intra-urban road network: A case study in the city center of Shanghai, China. J. Hydrol., 537, 138–145. https://doi.org/10.1016/j.jhydrol.2016.03.037, 2016.

Zhang, H., Jia, H., Liu, W., Wang, J., Xu, D., Li, S., and Liu, X., 2023. Spatiotemporal Information Mining for Emergency Response of Urban Flood Based on Social Media and Remote Sensing Data. Remote Sens., 15, 4301. https://doi.org/10.3390/rs15174301, 2023.

Zhao, J., Zhang, C., Wang, J., Abbas, Z., and Zhao, Y.: Machine learning and SHAP-based susceptibility assessment of storm flood in rapidly urbanizing areas: a case study of Shenzhen, China. Geomat. Nat. Hazards Risk, 15(1). https://doi.org/10.1080/19475705.2024.2311889, 2024.

Zhang, Q., Li, C., Wen, D., Kang, J., Chen, T., Zhang, B., Hu, Y., and Yin, J.: Global South shows higher urban flood exposures than the Global North under current and future scenarios. Commun. Earth Environ., 6, 594. https://doi.org/10.1038/s43247-025-02585-7, 2025.